Geometric Numerical Integration
Ernst Hairer
TU München
January – February 2010

Lecture 5: Long-time behavior of wave equations

Table of contents

We first extend the technique of modulated Fourier expansion to problems with several high frequencies, which can be resonant or non-resonant. An extension to infinitely many non-resonant high frequencies permits to obtain interesting results on the long-time behavior of nonlinearly perturbed wave equations.

1 Several high frequencies

We consider Hamiltonians of the form

$$H(x,\dot x) = \frac{1}{2}\sum_{j=0}^{\ell}\Big(\|\dot x_j\|^2 + \omega_j^2\,\|x_j\|^2\Big) + U(x), \tag{1}$$

where $x = (x_0, x_1, \ldots, x_\ell)$ with $x_j \in \mathbb{R}^{d_j}$, $\omega_j = \lambda_j/\varepsilon$ with $\lambda_0 = 0$, distinct $\lambda_j > 0$, and small $\varepsilon > 0$. After rescaling ε we may assume $\lambda_j \geq 1$ for all j. The equations of motion are a system of second-order differential equations

$$\ddot x = -\Omega^2 x + g(x), \tag{2}$$

where $\Omega = \mathrm{diag}(\omega_j I)$ with the frequencies $\omega_j = \lambda_j/\epsilon$ and $g(x) = -\nabla U(x)$. As suitable numerical methods we consider again the class of exponential (trigonometric) integrators with filter functions ψ and ϕ, studied in Lecture 4.

We are interested in the long-time near-conservation of the total energy $H(x, \dot{x})$ and the oscillatory energies

$$I_j(x, \dot{x}) = \frac{1}{2}\Big(\|\dot{x}_j\|^2 + \frac{\lambda_j^2}{\epsilon^2} \|x_j\|^2 \Big) \qquad \text{for} \qquad j \geq 1 \tag{3}$$

or suitable linear combinations thereof. Benettin, Galgani & Giorgilli[1] have shown that the quantities

$$I_\mu(x, \dot{x}) = \sum_{j=1}^{\ell} \frac{\mu_j}{\lambda_j} I_j(x, \dot{x}) \tag{4}$$

are approximately preserved over long times along solutions with bounded energy (independent of ε) if the potential $U(x)$ is analytic and $\mu = (\mu_1, \ldots, \mu_\ell)$ is orthogonal to the *resonance module*

$$\mathcal{M} = \{k \in \mathbb{Z}^\ell : k_1\lambda_1 + \ldots + k_\ell\lambda_\ell = 0\}, \tag{5}$$

and if a diophantine non-resonance condition holds outside $\mathcal{M}$. Since $\mu = \lambda$ is orthogonal to $\mathcal{M}$, the total oscillatory energy $\sum_{j=1}^{\ell} I_j(x, \dot{x})$ of the system is always approximately preserved.

Example 1 To illustrate the conservation of the various energies, we consider a Hamiltonian (1) with $\ell = 3$, $\lambda = (1, \sqrt{2}, 2)$ and we assume that the dimensions of x_j are all 1 with the exception of that of $x_1 = (x_{1,1}, x_{1,2})$ which is 2. The resonance module is then given by $\mathcal{M} = \{(k_1, 0, k_3)\,;\, k_1 + 2k_3 = 0\}$. We take $\epsilon^{-1} = \omega = 70$, the potential

$$U(x) = (0.05 + x_{1,1} + x_{1,2} + x_2 + 2.5\, x_3)^4 + \frac{1}{8}x_0^2\, x_{1,1}^2 + \frac{1}{2}x_0^2, \tag{6}$$

and $x(0) = (1, 0.3\epsilon, 0.8\epsilon, -1.1\epsilon, 0.7\epsilon)$, $\dot{x}(0) = (-0.2, 0.6, 0.7, -0.9, 0.8)$ as initial values. We consider I_μ for $\mu = (1, 0, 2)$ and $\mu = (0, \sqrt{2}, 0)$, which are both orthogonal to $\mathcal{M}$. In Figure 1 we plot the oscillatory energies for the individual components of the system. The corresponding frequencies are attached to the curves. We also plot the sum $I_1 + I_3$ of the three oscillatory energies corresponding to the resonant frequencies $1/\epsilon$ and $2/\epsilon$. We see that $I_1 + I_3$ as well as I_2 (which are I_μ for the above two vectors $\mu \perp \mathcal{M}$) are well conserved over long times up to small oscillations of size $\mathcal{O}(\epsilon)$. There is an energy exchange between the two components corresponding to the same frequency $1/\epsilon$, and also between components corresponding to resonant frequencies $1/\epsilon$ and $2/\epsilon$.

[1] G. Benettin, L. Galgani & A. Giorgilli, *Realization of holonomic constraints and freezing of high frequency degrees of freedom in the light of classical perturbation theory. II*, Commun. Math. Phys. 121 (1989) 557–601.

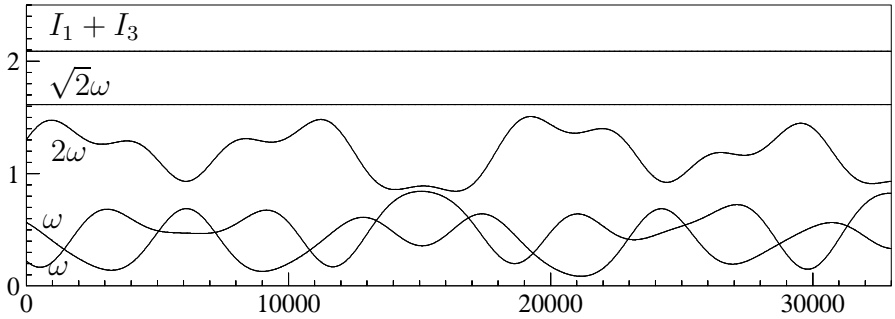

Figure 1: Oscillatory energies of the individual components (the frequencies $\lambda_j\omega = \lambda_j/\epsilon$ are indicated) and the sum $I_1 + I_3$ of the oscillatory energies corresponding to the resonant frequencies ω and 2ω.

Numerical Experiment. We take the exponential integrator (discussed in Lecture 4) with $\phi(\xi) = 1$ and $\psi(\xi) = \mathrm{sinc}(\xi)$, and we apply it with large step sizes so that $h\omega = h/\epsilon$ takes the values 1, 2, 4, and 8. Figure 2 shows the various oscillatory energies which can be compared to the exact values in Figure 1. For all step sizes, the oscillatory energy corresponding to the frequency $\sqrt{2}\omega$ and the sum

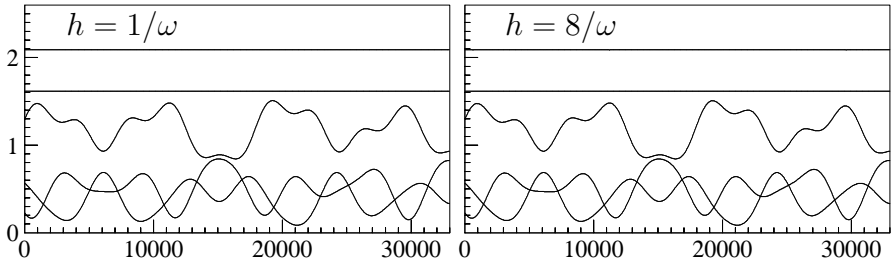

Figure 2: Oscillatory energies as in Figure 1 along the numerical solution, obtained with $\phi(\xi) = 1$ and $\psi(\xi) = \mathrm{sinc}(\xi)$.

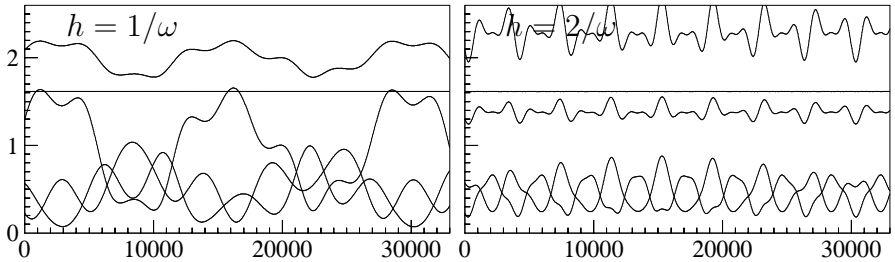

Figure 3: Oscillatory energies as in Figure 1 along the numerical solution, obtained with $\phi(\xi) = 1$ and $\psi(\xi) = \mathrm{sinc}^2(\xi/2)$.

$I_1 + I_3$ are well conserved on long time intervals. Oscillations in these expressions increase with h. The energy exchange between resonant frequencies is close to that of the exact solution. We have not plotted the total energy $H(x_n, \dot{x}_n)$ which is well conserved over long times.

We repeat this experiment with the method having filter functions $\phi(\xi) = 1$ and $\psi(\xi) = \mathrm{sinc}^2(\xi/2)$ (Figure 3). Only the oscillatory energy corresponding to $\sqrt{2}\omega$ is approximately conserved over long times. Neither the expression $I_1 + I_3$ nor the total energy (not shown) are conserved.

2 Multi-frequency modulated Fourier expansions

The technique of modulated Fourier expansion can be extended to the multi-frequency case by considering $k = (k_1, \ldots, k_\ell)$ as multi-index and by letting $k \cdot \omega = k_1\omega_1 + \ldots + k_\ell\omega_\ell$. We explain the main differences to the single-frequency case (Lecture 4) without giving technical details.

For a given vector $\lambda = (\lambda_1, \ldots, \lambda_\ell)$ and for the resonance module $\mathcal{M}$ defined by (5), we call k and $\widehat{k}$ equivalent (notation $k \sim \widehat{k}$) if $k \cdot \lambda = \widehat{k} \cdot \lambda$, i.e., $k - \widehat{k} \in \mathcal{M}$. We let $\mathcal{K}$ be a set of representatives of the equivalence classes which are chosen such that for each $k \in \mathcal{K}$ the sum $|k| = |k_1| + \ldots + |k_\ell|$ is minimal in the equivalence class $[k] = k + \mathcal{M}$, and with $k \in \mathcal{K}$, also $-k \in \mathcal{K}$.

Let us consider an exponential integrator (see Lecture 4) applied to the system (2). We write the numerical solution as $x_n = x_h(nh)$, where (formally)

$$x_h(t) \;=\; \sum_{k \in \mathcal{K}} e^{\mathrm{i}k\cdot\omega t} z_h^k(t) \tag{7}$$

with $\omega = \lambda/\varepsilon$. As in the single-frequency case we can construct smooth functions $z_h^k(t)$. We assume that the energy of the initial values is bounded independently of ϵ,

$$\frac{1}{2}\Big(\|\dot{x}(0)\|^2 + \|\Omega x(0)\|^2 \Big) \le E, \tag{8}$$

that $h/\varepsilon \ge c_0 > 0$, a numerical non-resonance condition, and bounds on the filter functions[2]. The dominant terms in each component are then bounded by

$$z_0^{\mathbf{0}} = \mathcal{O}(1), \qquad z_j^{\pm\langle j\rangle} = \mathcal{O}(\varepsilon) \quad \text{for} \quad j = 1, \ldots, \ell, \tag{9}$$

where $\langle j \rangle = (0, \ldots, 1, \ldots, 0)$ denotes the jth unit vector. All other functions are at least of size $h\varepsilon$ or ε^2.

[2]For a precise formulation of the assumptions, see Section XIII.9.2 of the monograph "Geometric Numerical Integration".

With $y^k(t) = e^{\mathrm{i}k\cdot\omega t} z_h^k(t)$ for $k \in \mathcal{K}$, where $z_h^k(t)$ are the modulation functions of (7), we denote $\mathbf{y} = (y^k)_{k\in\mathcal{K}}$. We introduce the extended potential

$$\mathcal{U}(\mathbf{y}) \;=\; U(\Phi y^0) + \sum_{s(\alpha)\sim 0} \frac{1}{m!}\, U^{(m)}(\Phi y^0)\big(\Phi y^{\alpha_1}, \ldots, \Phi y^{\alpha_m}\big), \tag{10}$$

where the sum is taken over all $m \geq 1$ and all multi-indices $\alpha = (\alpha_1, \ldots, \alpha_m)$ with $\alpha_j \in \mathcal{K}$ and $\alpha_j \neq \mathbf{0}$, for which $s(\alpha) = \sum_j \alpha_j \in \mathcal{M}$. The functions $y^k(t)$ then satisfy

$$\Psi^{-1}\Phi\, h^{-2}\mathcal{L}(hD)\, y^k \;=\; -\nabla_{y^{-k}}\mathcal{U}(\mathbf{y}), \tag{11}$$

where $\mathcal{L}(hD) = \mathrm{e}^{hD} - 2\,\cos(h\Omega) + \mathrm{e}^{hD}$. This system has almost-invariants that are related to the Hamiltonian H and the oscillatory energies I_μ with $\mu \perp \mathcal{M}$.

Momentum-type invariants of the modulation system. For $\mu \in \mathbb{R}^\ell$ we set

$$S_\mu(\tau)\,\mathbf{y} = (e^{\mathrm{i}k\cdot\mu\tau} y^k)_{k\in\mathcal{K}}, \qquad \tau \in \mathbb{R}$$

so that, by the multi-linearity of the derivative, the definition (10) yields

$$\mathcal{U}\big(S_\mu(\tau)\,\mathbf{y}\big) \;=\; U(\Phi y^0) + \sum_{s(\alpha)\sim 0} \frac{e^{\mathrm{i}s(\alpha)\cdot\mu\tau}}{m!}\, U^{(m)}(\Phi y^0)\big(\Phi y^{\alpha_1}, \ldots, \Phi y^{\alpha_m}\big). \tag{12}$$

If $\mu \perp \mathcal{M}$, then the relation $s(\alpha) \sim 0$ implies $s(\alpha)\cdot\mu = 0$, and hence the expression (12) is independent of τ. It therefore follows that

$$0 = \frac{d}{d\tau}\,\mathcal{U}\big(S_\mu(\tau)\,\mathbf{y}\big)\Big|_{\tau=0} = \sum_{k\in\mathcal{K}} \mathrm{i}\,(k\cdot\mu)\,(y^k)^{\mathsf{T}}\nabla_{y^k}\mathcal{U}(\mathbf{y}) \tag{13}$$

for all vectors $\mathbf{y} = (y^k)_{k\in\mathcal{K}}$. Multiplying the relation (11) with $\frac{\mathrm{i}}{\varepsilon}(-k\cdot\mu)\,\big(y^{-k}\big)^{\mathsf{T}}$ and summing over $k \in \mathcal{K}$, we obtain with (13) that, formally,

$$-\frac{\mathrm{i}}{\varepsilon}\sum_{k\in\mathcal{K}}(k\cdot\mu)(y^{-k})^{\mathsf{T}}\Psi^{-1}\Phi\, h^{-2}\mathcal{L}(hD)y^k = 0 \qquad \text{if} \quad \mu \perp \mathcal{M}.$$

Its dominant term is obtained for $k = \pm\langle j\rangle$, $j = 1, \ldots, \ell$,

$$-\frac{\mathrm{i}}{\varepsilon}\sum_{j=1}^{\ell}\mu_j\,\frac{\phi(h\omega_j)}{\psi(h\omega_j)}\,h^{-2}\Big((y_j^{-\langle j\rangle})^{\mathsf{T}}\mathcal{L}(hD)y_j^{\langle j\rangle} - (y_j^{\langle j\rangle})^{\mathsf{T}}\mathcal{L}(hD)y_j^{-\langle j\rangle}\Big) + \ldots = 0.$$

As in the single-frequency case, the left-hand expression turns out to be the time derivative of a function $\mathcal{I}_\mu^*\big(\mathbf{y}(t)\big)$ which after suitable truncation of the asymptotic

series gives $\frac{d}{dt}\mathcal{I}^*_\mu\big(\mathbf{y}(t)\big) \;=\; \mathcal{O}(h^N)$. This proves for $0 \le t \le T$

$$\mathcal{I}^*_\mu\big(\mathbf{y}(t)\big) \;=\; \mathcal{I}^*_\mu\big(\mathbf{y}(0)\big) \;+\; \mathcal{O}(th^N) \qquad \text{if} \quad \mu \perp \mathcal{M}. \tag{14}$$

Since $\mathcal{L}(hD)y_j^{\langle j\rangle}(t) = \mathcal{L}(hD)\big(\mathrm{e}^{\mathrm{i}\omega_j t} z_j^{\langle j\rangle}(t)\big) = 2\mathrm{i}\,\mathrm{sinc}(h\omega_j)\,h^2\omega_j\,\mathrm{e}^{\mathrm{i}\omega_j t}\,\dot z_j^{\langle j\rangle}(t) + \ldots$ and $I_j(x_n,\dot x_n) \;=\; 2\omega_j^2\,\|z_j^{\langle j\rangle}(nh)\|^2 \;+\; \mathcal{O}(\varepsilon)$, the invariant $\mathcal{I}^*_\mu\big(\mathbf{y}(t)\big)$ is close to a modified oscillatory energy (with $\sigma(\xi) = \mathrm{sinc}(\xi)\phi(\xi)/\psi(\xi)$)

$$\mathcal{I}^*_\mu\big(\mathbf{y}(nh)\big) \;=\; I^*_\mu(x_n,\dot x_n) + \mathcal{O}(\varepsilon), \quad I^*_\mu(x,\dot x) \;=\; \sum_{j=1}^{\ell} \sigma(h\omega_j)\,\frac{\mu_j}{\lambda_j}\,I_j(x,\dot x). \tag{15}$$

3 Long-time energy conservation

With $\sigma(\xi) = \mathrm{sinc}(\xi)\phi(\xi)/\psi(\xi)$ and $\omega_j = \lambda_j/\varepsilon$, we consider the modified total and oscillatory energies

$$\begin{aligned} H^*(x,\dot x) \;&=\; H(x,\dot x) + \sum_{j=1}^{\ell}\big(\sigma(h\omega_j) - 1\big)\,I_j(x,\dot x) \\ I^*_\mu(x,\dot x) \;&=\; \sum_{j=1}^{\ell} \sigma(h\omega_j)\,\frac{\mu_j}{\lambda_j}\,I_j(x,\dot x). \end{aligned} \tag{16}$$

Theorem 1 *Under a numerical non-resonance assumption and the usual condition on the filter functions $\psi(\xi)$ and $\phi(\xi)$ of an exponential integrator, its numerical solution satisfies, for H^* and I^*_μ defined by (16),*

$$\begin{aligned} H^*(x_n,\dot x_n) \;&=\; H^*(x_0,\dot x_0) + \mathcal{O}(h) \\ I^*_\mu(x_n,\dot x_n) \;&=\; I^*_\mu(x_0,\dot x_0) \;+ \mathcal{O}(h) \end{aligned} \qquad \textit{for} \qquad 0 \le nh \le h^{-N+1}$$

for $\mu \in \mathbb{R}^\ell$ with $\mu \perp \mathcal{M}$.

Proof. The proof of the statement for $I^*_\mu(x_n,\dot x_n)$ has been outlined in the previous section. That for the modified total Hamiltonian follows similar lines and is not presented. □

For $\sigma(\xi) = 1$ (or equivalently $\psi(\xi) = \mathrm{sinc}(\xi)\phi(\xi)$) the modified energies H^* and I^*_μ are identical to the original energies H and I_μ of (1) and (4). The condition $\psi(\xi) = \mathrm{sinc}(\xi)\phi(\xi)$ is known to be equivalent to the symplecticity of the one-step method $(x_n,\dot x_n) \mapsto (x_{n+1},\dot x_{n+1})$, but its appearance in the above theorem is caused by a mechanism which is not in any obvious way related to symplecticity.

Explanation of the Numerical Experiment of Section 1. All numerical methods in Figures 2–3 satisfy the conditions of Theorem 1 for the step sizes considered.

In Figure 2 we have the (symplectic) method with $\phi(\xi) = 1$ and $\psi(\xi) = \mathrm{sinc}(\xi)$, which has $\sigma(\xi) = 1$, so that H and H^*, and I_μ and I^*_μ coincide. For all step sizes, the oscillatory energy I_2 corresponding to the non-resonant frequency $\sqrt{2}\omega$ and the sum $I_1 + I_3$ are well conserved on long time intervals, in accordance with Theorem 1. There is an exchange between the individual energies I_1 and I_3 corresponding to the resonant frequencies $\omega = 1/\varepsilon$ and $2/\varepsilon$.

In Figure 3 we use the method with $\phi(\xi) = 1$ and $\psi(\xi) = \mathrm{sinc}^2(\xi/2)$, for which $\sigma(\xi)$ is not identical to 1, and hence H and H^*, and I_μ and I^*_μ do not coincide. The oscillatory energy $I_2 = \sigma_2^{-1} I^*_\mu$ with $\mu = (0, 1, 0) \perp \mathcal{M}$, which corresponds to the non-resonant frequency $\sqrt{2}\omega$, is approximately conserved over long times. Since Theorem 1 only states that the *modified* energies are well preserved, it is not surprising that neither $I_1 + I_3$ nor the original total energy H (not shown in the figure) are conserved. The modified energies H^* and $\sigma_1 I_1 + \sigma_3 I_3$ (not shown) are indeed well conserved.

Experiment with the Störmer–Verlet method. We repeat the experiment of Figure 1 with the Störmer–Verlet method. Recall that the maximal frequency of the system is $2\omega = 2/\varepsilon = 140$. Figure 4 shows a surprising behavior of the oscillatory energies. The energy I_2 (corresponding to $\omega_2 = \sqrt{2}/\varepsilon$) and the sum $I_1 + I_3$ (corresponding to the two components with $\omega = 1/\varepsilon$ and the resonant one with $\omega = 2/\varepsilon$) are well conserved.

For the step size $h = 0.15/\omega$, the oscillatory energy I_3 is nearly constant, and there is an exchange of energy between the two components corresponding to the same frequency ω. This can be explained by the fact, that the Störmer–Verlet method is identical to an exponential integrator applied to a system with modified frequencies $\widetilde{\omega}_j$ defined by $\sin(\frac{2}{h}\widetilde{\omega}_j) = \frac{1}{2}h\omega_j$. If ω_1 and $\omega_3 = 2\omega_1$ are resonant, this is no longer the case for the corresponding $\widetilde{\omega}_j$. The picture to the right of Figure 4 shows that rather small step sizes are needed to reproduce an energy exchange, and a much smaller step size to reproduce it correctly.

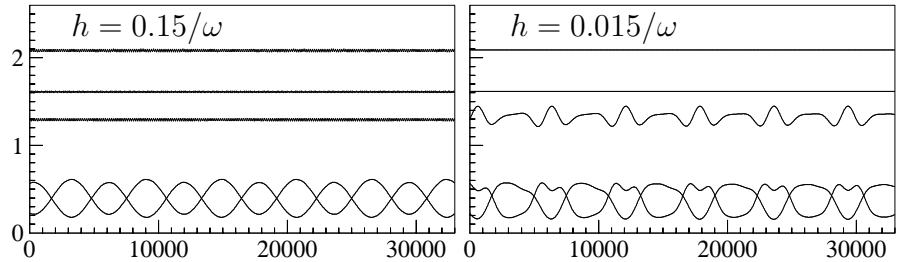

Figure 4: Oscillatory energies as in Figure 1 along the numerical solution of the Störmer–Verlet method.

4 Semi-linear wave equations

We consider the one-dimensional nonlinear wave equation

$$u_{tt} - u_{xx} + \rho u + g(u) = 0 \tag{17}$$

for $t > 0$ and $-\pi \leq x \leq \pi$ subject to periodic boundary conditions. We assume $\rho > 0$ and a nonlinearity g that is a smooth real function with $g(0) = g'(0) = 0$. We consider small initial data: in appropriate Sobolev norms, the initial values $u(\cdot, 0)$ and $u_t(\cdot, 0)$ are bounded by a small parameter ε. By rescaling u, this assumption could be rephrased as a $\mathcal{O}(1)$ initial datum but a small non-linearity.

The semi-linear wave equation (17) conserves several quantities along every solution $\big(u(x,t), v(x,t)\big)$, with $v = \partial_t u$. The *total energy* or Hamiltonian, defined for 2π-periodic functions u, v as

$$H(u,v) = \frac{1}{2\pi} \int_{-\pi}^{\pi} \left(\frac{1}{2} \Big(v^2 + (\partial_x u)^2 + \rho\, u^2 \Big)(x) + U\big(u(x)\big) \right) dx, \tag{18}$$

where the potential $U(u)$ is such that $U'(u) = g(u)$, and the *momentum*

$$K(u,v) = \frac{1}{2\pi} \int_{-\pi}^{\pi} \partial_x u(x)\, v(x)\, dx = -\sum_{j=-\infty}^{\infty} \mathrm{i}\, j\, u_{-j}\, v_j \tag{19}$$

are exactly conserved along every solution $\big(u(\cdot,t), v(\cdot,t)\big)$ of (17). Here, $u_j = \mathcal{F}_j u$ and $v_j = \mathcal{F}_j v$ are the Fourier coefficients in the series $u(x) = \sum_{j=-\infty}^{\infty} u_j \mathrm{e}^{\mathrm{i}jx}$ and correspondingly $v(x)$. Since we consider only real solutions, we note that $u_{-j} = \overline{u}_j$ and $v_{-j} = \overline{v}_j$. In terms of the Fourier coefficients, equation (17) reads

$$\partial_t^2 u_j + \omega_j^2 u_j + \mathcal{F}_j g(u) = 0, \qquad j \in \mathbb{Z}, \tag{20}$$

with the frequencies

$$\omega_j = \sqrt{\rho + j^2}.$$

The *harmonic actions*

$$I_j(u,v) = \frac{1}{2} \Big(\omega_j\, |u_j|^2 + \frac{1}{\omega_j}\, |v_j|^2 \Big), \tag{21}$$

for which we note $I_{-j} = I_j$, are conserved for the linear wave equation, that is, for $g(u) \equiv 0$. In the semi-linear equation (17), they turn out to remain constant up to small deviations over long times for almost all values of $\rho > 0$, when the initial data are smooth and small. Such a result is proved in Bambusi [3], Bourgain [4], and

[3] D. Bambusi, *Birkhoff normal form for some nonlinear PDEs*, Comm. Math. Phys. 234 (2003) 253–285

[4] J. Bourgain, *Construction of approximative and almost periodic solutions of perturbed linear Schrödinger and wave equations*, Geom. Funct. Anal. 6 (1996) 201–230

Cohen, Hairer, and Lubich [5]. We recall the precise statement of this result, because this will help to understand related assumptions for the numerical discretizations.

We work with the Sobolev space, for $s \geq 0$,

$$H^s = \{v \in L^2(\mathbb{T}) : \|v\|_s < \infty\}, \qquad \|v\|_s = \Big(\sum_{j=-\infty}^{\infty} \omega_j^{2s} \, |v_j|^2 \Big)^{1/2},$$

where v_j denote the Fourier coefficients of a 2π-periodic function v. For the initial position and velocity we assume that for suitably large s and small ε,

$$\Big(\|u(\cdot,0)\|_{s+1}^2 + \|v(\cdot,0)\|_s^2 \Big)^{1/2} \leq \varepsilon. \tag{22}$$

Theorem 2 *Under a suitable non-resonance condition on the ω_j, and the assumption (22) on the initial data with $s \geq \sigma + 1$, the estimate*

$$\sum_{\ell=0}^{\infty} \omega_\ell^{2s+1} \, \frac{|I_\ell(t) - I_\ell(0)|}{\varepsilon^2} \leq C\varepsilon \qquad \textit{for} \qquad 0 \leq t \leq \varepsilon^{-N+1}$$

with $I_\ell(t) = I_\ell\big(u(\cdot,t), v(\cdot,t)\big)$ holds with a constant C which depends on s and N, but is independent of ε and t.

The smallness of the initial data, which implies that the non-linearity is small compared to the linear terms, is essential for our analysis. Since we do not impose any further restrictions on the non-linearity, such an assumption permits to avoid blow-up in finite time.

5 Spectral semi-discretization in space

For the numerical solution of (17) we first discretize in space (method of lines) and then in time. We consider pseudo-spectral semi-discretization in space with equidistant collocation points $x_k = k\pi/M$ (for $k = -M, \ldots, M-1$). This yields an approximation in form of real-valued trigonometric polynomials

$$u^M(x,t) = {\sum_{|j| \leq M}}' q_j(t) \mathrm{e}^{\mathrm{i}jx}, \qquad v^M(x,t) = {\sum_{|j| \leq M}}' p_j(t) \mathrm{e}^{\mathrm{i}jx} \tag{23}$$

where the prime indicates that the first and last terms in the sum are taken with the factor $1/2$. We have $p_j(t) = \frac{d}{dt} q_j(t)$, and the $2M$-periodic coefficient vector

[5] D. Cohen and E. Hairer and C. Lubich, *Long-time analysis of nonlinearly perturbed wave equations via modulated Fourier expansions*, Arch. Ration. Mech. Anal. 187 (2008) 341–368

$q(t) = (q_j(t))$ is a solution of the $2M$-dimensional system of ordinary differential equations

$$\frac{d^2q}{dt^2} + \Omega^2 q = f(q) \qquad \text{with} \qquad f(q) = -\mathcal{F}_{2M} g(\mathcal{F}_{2M}^{-1} q). \tag{24}$$

The matrix Ω is diagonal with entries ω_j for $|j| \le M$, and $\mathcal{F}_{2M}$ denotes the discrete Fourier transform:

$$\big(\mathcal{F}_{2M} w\big)_j = \frac{1}{2M} \sum_{k=-M}^{M-1} w_k \, \mathrm{e}^{-\mathrm{i} j x_k}.$$

Since the components of the nonlinearity in (24) are of the form

$$f_j(q) = -\frac{\partial}{\partial q_{-j}} V(q) \qquad \text{with} \qquad V(q) = \frac{1}{2M} \sum_{k=-M}^{M-1} U\big((\mathcal{F}_{2M}^{-1} q)_k\big)\,,$$

we are concerned with a finite-dimensional complex Hamiltonian system with energy

$$H_M(q,p) = \frac{1}{2} {\sum_{|j|\le M}}' \Big(|p_j|^2 + \omega_j^2 \, |q_j|^2 \Big) + V(q), \tag{25}$$

which is exactly conserved along the solution $\big(q(t), p(t)\big)$ of (24) with $p(t) = dq(t)/dt$. We further consider the actions (for $|j| \le M$) and the momentum

$$I_j(q,p) = \frac{1}{2}\Big(\omega_j \, |q_j|^2 + \frac{1}{\omega_j} \, |p_j|^2\Big), \qquad K(q,p) = -{\sum_{|j|\le M}}'' \mathrm{i}\, j \, q_{-j} p_j, \tag{26}$$

where the double prime indicates that the first and last terms in the sum are taken with the factor $1/4$. The definition of these expressions is motivated by the fact that they agree with the corresponding quantities of Section 4 along the trigonometric polynomials u^M, v^M (with the exception of $I_{\pm M}$, where a factor 4 must be included to get a unified formula). Since we are concerned with real approximations (23), the Fourier coefficients satisfy $q_{-j} = \overline{q}_j$ and $p_{-j} = \overline{p}_j$, so that also $I_{-j} = I_j$.

On the space of $2M$-periodic sequences $q = (q_j)$ we consider the weighted norm

$$\|q\|_s = \Big({\sum_{|j|\le M}}'' \omega_j^{2s} |q_j|^2 \Big)^{1/2}, \tag{27}$$

which is defined such that it equals the H^s norm of the trigonometric polynomial with coefficients q_j. We assume that the initial data $q(0)$ and $p(0)$ satisfy a

condition corresponding to (22):

$$\Big(\|q(0)\|_{s+1}^2 + \|p(0)\|_s^2 \Big)^{1/2} \le \varepsilon. \tag{28}$$

The following result [6] is the analogue of Theorem 2 of the previous section.

Theorem 3 *Under a suitable non-resonance condition on the ω_j (which involves a parameter σ), and the assumption (28) of small initial data with $s \ge \sigma + 1$, the near-conservation estimates*

$$\begin{aligned} \sum_{\ell=0}^{M} \omega_\ell^{2s+1} \, \frac{|I_\ell(t) - I_\ell(0)|}{\varepsilon^2} &\le C\varepsilon \\ \frac{|K(t) - K(0)|}{\varepsilon^2} &\le C\, t\, \varepsilon M^{-s-1} \end{aligned} \qquad \text{for} \qquad 0 \le t \le \varepsilon^{-N+1}$$

for actions $I_\ell(t) = I_\ell\big(q(t), p(t)\big)$ and momentum $K(t) = K\big(q(t), p(t)\big)$ hold with a constant C that depends on s and N, but is independent of ε, M, and t.

Since the expression $\sum_{\ell=0}^{M} \omega_\ell^{2s+1} I_\ell(t)$ is essentially (up to the factors in the boundary terms) equal to the squared $H^{s+1} \times H^s$ norm of the solution $\big(q(t), p(t)\big)$, Theorem 3 implies long-time spatial regularity:

$$\Big(\|q(t)\|_{s+1}^2 + \|p(t)\|_s^2 \Big)^{1/2} \le \varepsilon(1 + C\varepsilon) \qquad \text{for} \qquad t \le \varepsilon^{-N+1}. \tag{29}$$

Theorems 2 and 3 have been included as a motivation of our results. They will not be used in the following.

Example 2 In our numerical experiments we consider the Sine–Gordon equation, which is of the form (17) with $\rho = 0$ and $g(u) = \sin u$. We use initial data[7]

$$u(x,0) = \pi, \quad \partial_t u(x,0) = 1.4\big(\sin(\pi x) + 0.005\, \pi^2 x(2-x)\big)$$

for $0 \le x \le 2$. The spatial discretization is (24) with dimension $2M = 2^7$. Considered as 2-periodic functions, the initial data $\partial_t u(\cdot, 0)$ has a jump discontinuity in the first derivative. The assumption (28) is therefore satisfied for $s < 1.5$.

Figure 5 shows the total energy (black bold line) and the harmonic actions I_k (for even k in red, and for odd k in blue lines) along the exact solution of the problem. To see a more interesting dynamics, we have chosen relatively large initial functions (otherwise only straight lines could be seen).

[6] E. Hairer and C. Lubich, *Spectral semi-discretisations of weakly nonlinear wave equations over long times*, Found. Comput. Math. 8 (2008) 319–334.

[7] All our numerical experiments are done for a normalization $x \in [0, 2]$, so that the frequencies ω_j become $\omega_j = j\pi$ for $\rho = 0$.

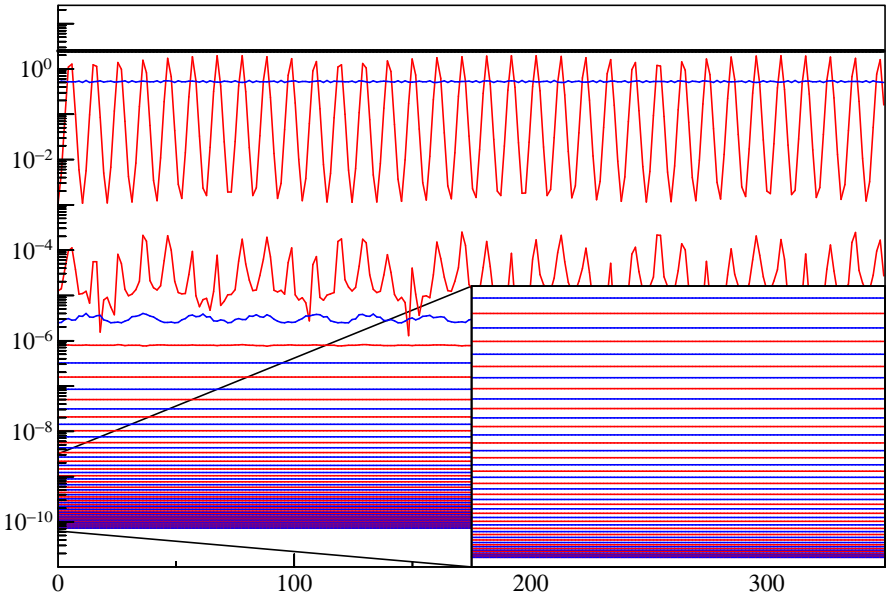

Figure 5: Actions and total energy (upper bold line) along the exact solution of the Sine–Gordon equation (data of Example 2).

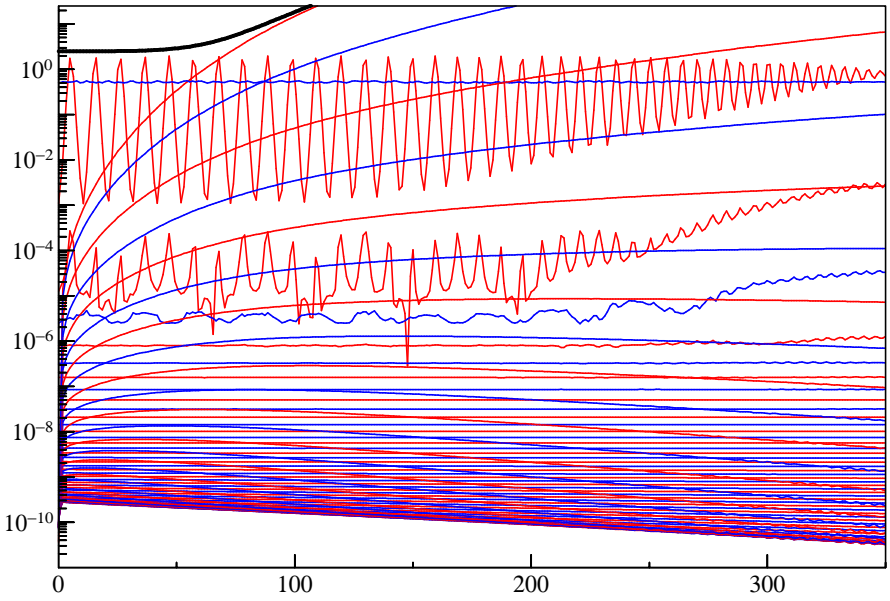

Figure 6: Actions and total energy (upper bold line) along the numerical solution of DOPRI5, $Atol = Rtol = 4 \cdot 10^{-4}$, average CFL number 1.13.

We apply an explicit Runge–Kutta method in the variable stepsize implementation DOPRI5, with local error tolerances *Atol* = *Rtol* = $4 \cdot 10^{-4}$. The program chose $62\,267$ accepted steps for the integration over the interval $0 \le t \le 350$, which corresponds to an average stepsize $\overline{h} = 0.00562$ and average CFL number $\overline{h}\omega_M = 1.13$. In Figure 6 we plot the actions I_j of (21), and the total energy H_M of (25) along the numerical solution. Even on the short time intervals the actions with values below the tolerance are not at all conserved. There is a substantial drift in all the quantities (also in the total energy) over longer time intervals.

6 Full discretizations – main results

We consider trigonometric (exponential) time integrators, which give the exact solution for linear problems (24) with $f(q) = 0$, and reduce to the Störmer–Verlet / leapfrog method for (24) with $\Omega = 0$:

$$\begin{aligned} q^{n+1} - 2\cos(h\Omega)\, q^n + q^{n-1} &= h^2 \Psi\, f(\Phi q^n) \\ 2h\,\mathrm{sinc}(h\Omega)\, p^n &= q^{n+1} - q^{n-1}, \end{aligned} \tag{30}$$

where $\Psi = \psi(h\Omega)$ and $\Phi = \phi(h\Omega)$ with filter functions ψ and ϕ that are bounded, even, and satisfy $\psi(0) = \phi(0) = 1$. We have the following results.[8]

Theorem 4 *Under the symplecticity condition $\psi(\xi) = \mathrm{sinc}(\xi)\phi(\xi)$, under a suitable non-resonance conditions (involving a parameter σ), and under the assumption (28) of small initial data with $s \ge \sigma + 1$ for $(q^0, p^0) = \big(q(0), p(0)\big)$, the near-conservation estimates*

$$\begin{aligned} \frac{|H_M(q^n,p^n) - H_M(q^0,p^0)|}{\varepsilon^2} &\le C\varepsilon \\ \frac{|K(q^n,p^n) - K(q^0,p^0)|}{\varepsilon^2} &\le C\big(\varepsilon + M^{-s} + \varepsilon t M^{-s+1}\big) \\ \sum_{\ell=0}^{M} \omega_\ell^{2s+1}\, \frac{|I_\ell(q^n,p^n) - I_\ell(q^0,p^0)|}{\varepsilon^2} &\le C\varepsilon \end{aligned}$$

for energy, momentum and actions hold for long times $0 \le t = nh \le \varepsilon^{-N+1}$ with a constant C which depends on s and N, but is independent of the small parameter ε, the dimension $2M$ of the spatial discretization, the time stepsize h, and the time $t = nh$.

[8] D. Cohen, E. Hairer and C. Lubich, *Conservation of energy, momentum and actions in numerical discretizations of nonlinear wave equations*, Numer. Math. 110 (2008) 113–143.

In addition we obtain that the original Hamiltonian H of (18) along the trigonometric interpolation polynomials $\big(u^n(x), v^n(x)\big)$ with Fourier coefficients (q_j^n, p_j^n) satisfies the long-time near-conservation estimate

$$\frac{|H(u^n, v^n) - H(u^0, v^0)|}{\varepsilon^2} \leq C\varepsilon \qquad \text{for} \qquad 0 \leq nh \leq \varepsilon^{-N+1}\,.$$

The proof of Theorem 4 is based on the idea of interpolating the numerical solution by a function where different time scales are well separated (modulated Fourier expansion). This is done by the ansatz

$$\widetilde{q}_h(t) = \sum_{\mathbf{k}} \mathrm{e}^{\mathrm{i}(\mathbf{k}\cdot\omega)t} z^{\mathbf{k}}(\varepsilon t), \tag{31}$$

approximating the numerical solution q^n at $t = nh$. It s a (truncated) series of products of $\mathrm{e}^{\mathrm{i}\omega_j t}$ (oscillations with respect to the fast time t) with coefficient functions that are smooth in the slow time $\tau = \varepsilon t$. The proof then proceeds as follows:

- Proving existence of smooth functions $z^{\mathbf{k}}(\tau)$ with derivatives bounded independently of ε (on intervals of length ε^{-1}). This is the technically difficult part and requires non-resonance conditions and a careful truncation of the series.
- Establishing a Hamiltonian structure and the existence of formal invariants in the differential and algebraic equations for the functions $z^{\mathbf{k}}(\tau)$.
- Proving closeness (on intervals of length ε^{-1}) of the formal invariants to actions I_ℓ, to the total energy H, and to the momentum K.
- Stretching from short to long intervals of length ε^{-N+1} by patching together previous results along an invariant.

New difficulties arise due to the large number of independent frequencies (all estimates have to be independent of M), the analytic non-resonance condition, and the necessity of working with suitable Sobolev norms.

Numerical experiments. We study the effect of numerical resonance at the problem of Example 2 (notice that the frequencies are $\omega_j = j\pi$ for $j = 0, 1, \ldots, M$). We start with the method of Gautschi for which $\psi(\xi) = \mathrm{sinc}^2(\xi/2)$ and $\phi(\xi) = 1$. We choose step sizes close to $h = 0.1$ so that $h\omega_{10} = \pi$. Figure 7 shows that the harmonic energy of the 10 th Fourier mode explodes rapidly and causes a wrong behavior of the solution. Surprisingly, for the case of exact resonance we have a relative good behavior.

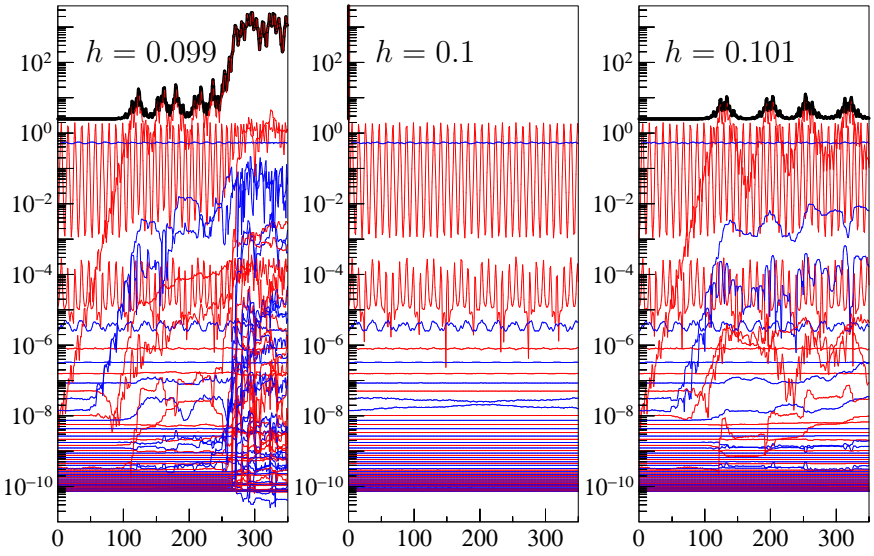

Figure 7: Illustration of numerical resonance; method of Gautschi with $\psi(\xi) = \mathrm{sinc}^2(\xi/2)$ and $\phi(\xi) = 1$.

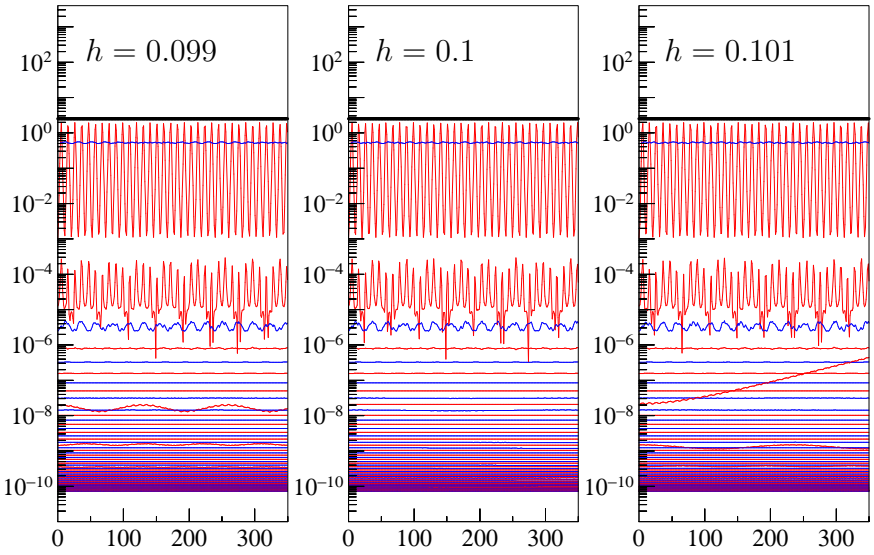

Figure 8: Illustration of numerical resonance; method of Deuflhard with $\psi(\xi) = \mathrm{sinc}(\xi)$ and $\phi(\xi) = 1$.

The resonance behaviour depends strongly on the choice of the filter functions. For the method of Deuflhard (with $\psi(\xi) = \mathrm{sinc}(\xi)$ and $\phi(\xi) = 1$) the conservation of total energy and harmonic actions is much improved (see Figure 8). Only the

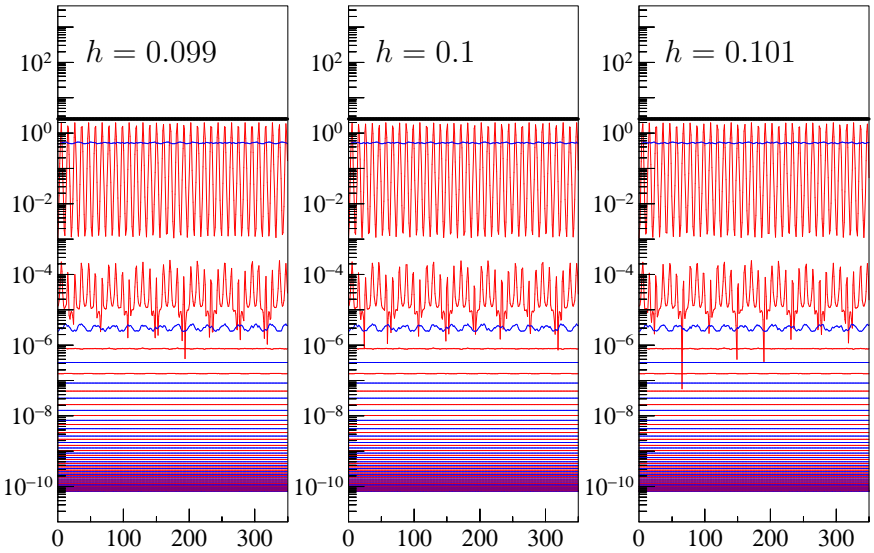

Figure 9: Illustration of numerical resonance; method of García-Archilla & al. with $\psi(\xi) = \mathrm{sinc}(\xi)\phi(\xi)$ and $\phi(\xi) = \mathrm{sinc}(\xi)$.

harmonic energy corresponding to the 10 th mode and later also that for the 20 th mode show a drift. Still better is the method of Figure 9.

7 The Störmer–Verlet / leapfrog discretization

The leapfrog discretization of (24) reads, in the two-step formulation,

$$q^{n+1} - 2\,q^n + q^{n-1} = h^2\big(-\Omega^2 q^n + f(q^n)\big), \tag{32}$$

with the velocity approximation p^n given by

$$2h\,p^n = q^{n+1} - q^{n-1}. \tag{33}$$

The starting value is chosen as $q^1 = q^0 + hp^0 + \frac{h^2}{2}\,f(q^0)$. Conservation properties of this method will be obtained by reinterpreting it as a trigonometric method (30) with modified frequencies $\widetilde{\omega}_j$ satisfying $1 - \frac{1}{2}h^2\omega_j^2 = \cos(h\widetilde{\omega}_j)$, that is,

$$\sin\Big(\frac{1}{2}\,h\widetilde{\omega}_j\Big) = \frac{1}{2}\,h\omega_j. \tag{34}$$

This is possible as long as $h\omega_j \le 2$. Under the stepsize restriction $h\omega_M \le c < 2$ the product $h\widetilde{\omega}_j$ cannot be close to an integral multiple of π, and we have

$$\omega_j \le \widetilde{\omega}_j \le C\omega_j,$$

where C depends only on c. Hence, the assumption (28) of small initial data is satisfied with the same exponent s for the weighted norms defined with $\widetilde{\omega}_j$ or with ω_j. We can therefore apply Theorem 4 in the transformed variables, defined by

$$\widetilde{q}^n = \chi(h\widetilde{\Omega})\, q^n, \qquad \widetilde{p}^n = \chi(h\widetilde{\Omega})^{-1} p^n$$

with $\chi^2(\xi) = \mathrm{sinc}(\xi)$ (notice that the corresponding exponential integrator has $\psi(\xi) = \chi(\xi)$ and $\phi(\xi) = \chi^{-1}(\xi)$ and is symplectic) and thus obtain, for example,

$$\sum_{\ell=0}^{M} \widetilde{\omega}_\ell^{2s+1} \, \frac{|\widetilde{I}_\ell(\widetilde{q}^n, \widetilde{p}^n) - \widetilde{I}_\ell(\widetilde{q}^0, \widetilde{p}^0)|}{\varepsilon^2} \le C\varepsilon \qquad \text{for} \qquad 0 \le t \le \varepsilon^{-N+1}.$$

It follows from the computations of the last section in Lecture 4 that the harmonic actions $\widetilde{I}_\ell(\widetilde{q}^n, \widetilde{p}^n)$ are related to $I_\ell(q^n, p^n)$ by

$$\widetilde{I}_\ell(\widetilde{q}^n, \widetilde{p}^n) \;=\; \Big(\frac{\widetilde{\omega}_\ell \, \chi^2(h\omega_\ell)}{\omega_\ell}\Big)\Big(I_\ell(q^n, p^n) + \frac{\gamma(h\omega_j)}{2\omega_j}\, \|p_\ell^n\|^2\Big).$$

where

$$\gamma(h\omega) = \frac{(h\omega/2)^2}{1 - (h\omega/2)^2}$$

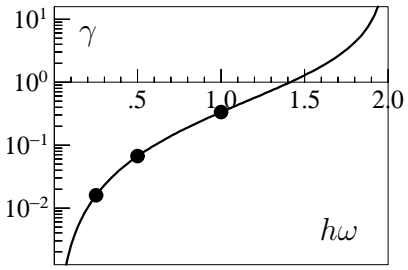

This implies that for the modified energies

$$I_\ell^*(q^n, p^n) \;=\; I_\ell(q^n, p^n) + \frac{\gamma(h\omega_j)}{2\omega_j}\, \|p_\ell^n\|^2$$

we have the estimate

$$\sum_{\ell=0}^{M} \omega_\ell^{2s+1} \, \frac{|I_\ell^*(q^n, p^n) - I_\ell^*(q^0, p^0)|}{\varepsilon^2} \le C\varepsilon \qquad \text{for} \qquad 0 \le t \le \varepsilon^{-N+1}. \quad (35)$$

Numerical experiment. We apply the leapfrog method to the problem of Example 5 with stepsize $h = 0.009$, so that the CFL number $h\omega_M \approx 1.81$ is close to the linear stability limit. In Figure 10 we observe that the harmonic actions I_ℓ are very well reproduced for small values of ℓ. For large values of ℓ, in particular when they are close to M, oscillations with large relative amplitude proportional to $\gamma(h\omega_\ell)$ are observed, but there is no drift in actions and energy. For reason of comparison, we include again the picture for the exact values (actually obtained with an exponential integrator).

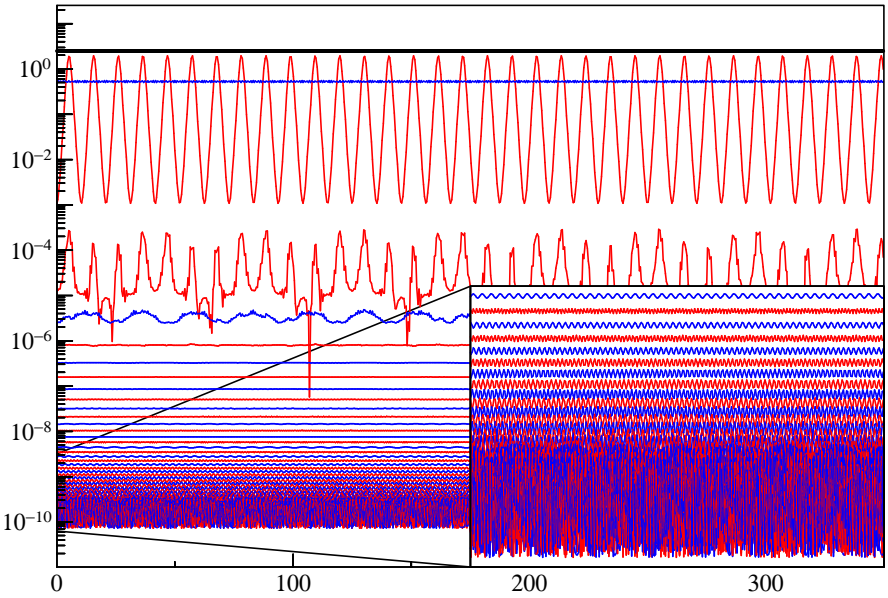

Figure 10: Actions and total energy (upper bold line) along the numerical of the Stömer–Verlet / leapfrog method (problem of Example 2).

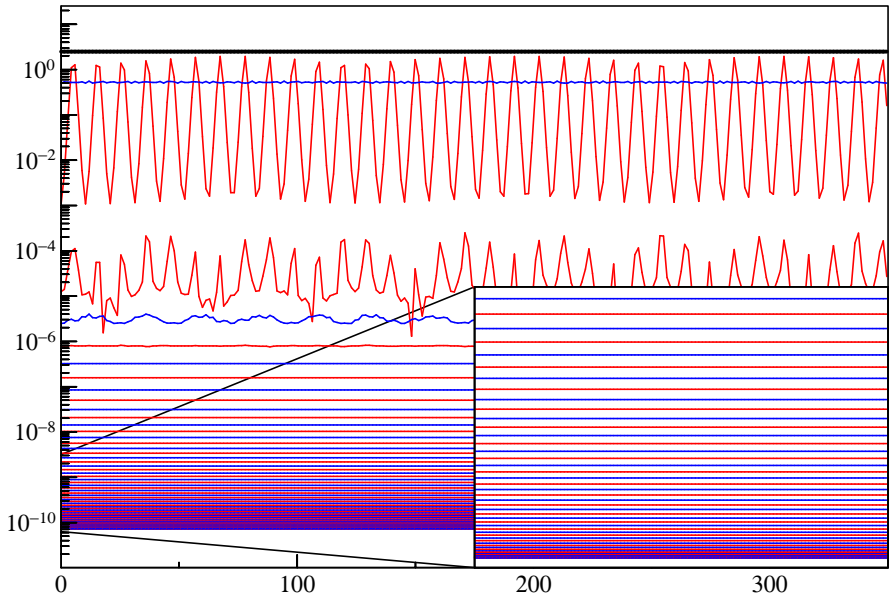

Figure 11: Actions and total energy (upper bold line) along the exact solution of the Sine–Gordon equation (data of Example 2).